2.7 Strong WW Scattering

In this section we examine how well an e^+e^- linear collider with a center-of-mass energy of 500–1500 GeV can study the strongly interacting Higgs sector. We also compare the estimated sensitivity of such a collider with that of the LHC.

2.7.1 The Reaction $e^+e^- \to W^+W^-$

Strong electroweak symmetry breaking affects the reaction $e^+e^- \to W^+W^-$ through anomalous couplings at the $W^+W^-\gamma$ and W^+W^-Z vertices and through enhancements in $W_{\rm L}^+W_{\rm L}^-$ production due to $I = J = 1$ resonances. Here we have used the symbol W_L to denote a longitudinally polarized W boson. Anomalous couplings at the three-gauge boson vertices are related to the chiral Lagrangian parameters L_{9L} and L_{9R} [77]. A technipion form factor F_T is used to parameterize [89] the strong $W_{\rm L}^+W_{\rm L}^-$ interaction in the $I = J = 1$ state; it is analogous to the rho–dominated pion form factor in $e^+e^- \to \pi^+\pi^-$.

Whether one is measuring trilinear vector boson couplings or searching for an enhancement in $W_{\rm L}^+W_{\rm L}^-$ production, the experimental goal is the same: disentangle the W^+W^- polarization states, and in particular isolate the polarization state $W_{\rm L}^+W_{\rm L}^-$. We shall describe the results of a study that utilizes a final-state helicity analysis of all observable final-state variables in order to isolate $W_{\rm L}^+W_{\rm L}^-$ production [3].

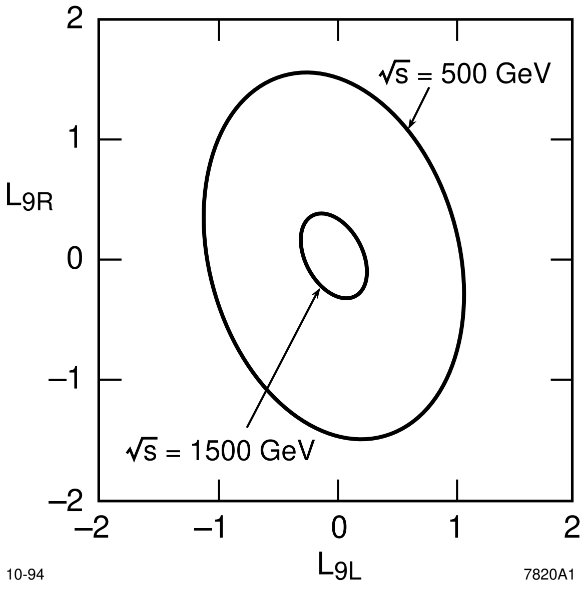

Figure 2.40: The 95% confidence level contours for L_{9L} and L_{9R} at $\sqrt{s} = 500$ GeV with 80 fb^{-1}, and at $\sqrt{s} = 1500$ GeV with 190 fb^{-1}. The outer contour is for $\sqrt{s} = 500$ GeV. In each case the initial state electron polarization is 90%.

The maximum likelihood method is used to fit for chiral Lagrangian parameters or for the real and imaginary parts of the technipion form factor. Figure 2.40 shows the 95% confidence level contours for the chiral Lagrangian parameters L_{9L} and L_{9R} at $\sqrt{s} = 500$ GeV and at $\sqrt{s} = 1500$ GeV. The parameters L_{9L} and L_{9R} are normalized such that values of $\mathcal{O}(1)$ are expected if the Higgs sector is strongly interacting.

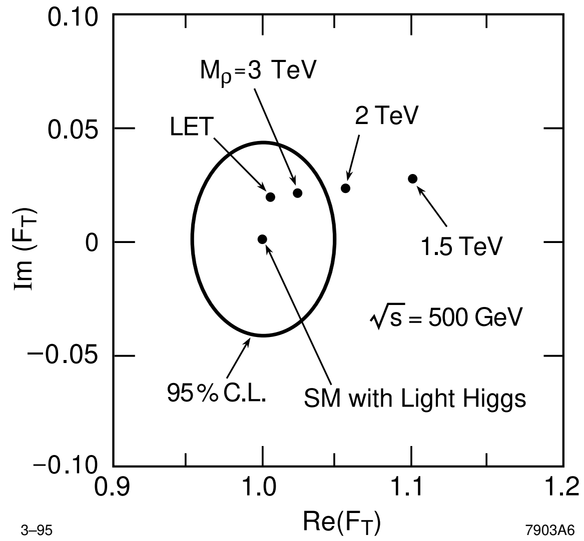

Figure 2.41: 95% confidence level contours for the real and imaginary parts of F_T at $\sqrt{s} = 500$ GeV with 80 fb^{-1}. The values of F_T for various technirho masses are indicated.

Figure 2.41 shows the 95% confidence level contour for the real and imaginary parts of F_T at $\sqrt{s} = 500$ GeV. The use of beam polarization is essential to obtain a strong constraint on $\mathrm{Im}(F_T)$. Also indicated are values of F_T for various technirho masses. The infinite technirho mass point is labelled Low Energy Theorem (LET) since in this limit there is residual $W_L^+W_L^-$ scattering described by the same low energy theorems that govern low energy $\pi^+\pi^-$ scattering. We see that the NLC at $\sqrt{s} = 500$ GeV can exclude technirho masses up to about 2.5 TeV and can discover technirho resonances with masses of more than 1.5 TeV. The significance of the 1.5 TeV technirho signal would be 6.7σ. A 1.0 TeV technirho would produce a 17.7σ signal. For comparison, the minimal technicolor model predicts a technirho mass of about 2.0 TeV.

Figure 2.42 contains confidence level contours for the real and imaginary parts of F_T at $\sqrt{s} = 1500$ GeV. The non-resonant LET point is well outside the light Higgs 95% confidence level region and corresponds to a 4.5σ signal. The labeling of points here deserves some comment. We use the model of [89] to describe the form factor F_T. In this model, as the vector resonance mass is taken to infinity, its effect on the form factor decreases, and what is left behind is the residual scattering predicted by the LET. The values for high-mass technirho indicate this decoupling. With this understanding, the 6 TeV, 4 TeV and 3 TeV

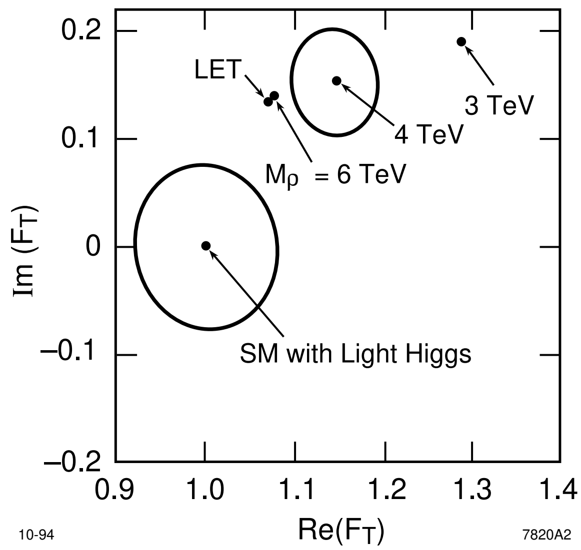

Figure 2.42: Confidence level contours for the real and imaginary parts of F_T at $\sqrt{s} = 1500$ GeV with 190 fb^{-1}. The contour about the light Higgs value of $F_T = (1, 0)$ is 95% confidence level and the contour about the $M_\rho = 4$ TeV point is 68% confidence level.

technirho points correspond to 4.8σ, 6.5σ, and 11σ signals, respectively. A 2 TeV technirho would produce a 37σ signal.

It might appear that the value of F_T, and hence the significance of technirho signals, would be very sensitive to the technirho width when $\sqrt{s}$ is much less than the technirho mass. In the model we have considered, however, this is not true. The results presented above were obtained assuming that $\Gamma_\rho/M_\rho = 0.22$. If, for example, the technirho width is reduced to $\Gamma_\rho/M_\rho = 0.03$ then the 1 TeV signal at $\sqrt{s} = 500$ GeV is reduced from 17.7σ to 16.3σ, the 1.5 TeV signal at $\sqrt{s} = 500$ GeV is reduced from 6.7σ to 6.4σ, and the 4 TeV signal at $\sqrt{s} = 1500$ GeV is reduced from 6.5σ to 6.3σ.

2.7.2 The Reaction $e^+e^- \to \nu\overline{\nu}W^+W^-$and $\nu\overline{\nu}$ZZ

The important gauge boson scattering processes $W_{\rm L}^+W_{\rm L}^- \to W_{\rm L}^+W_{\rm L}^-$ and $W_{\rm L}^+W_{\rm L}^- \to Z_LZ_L$ are studied at the NLC with the reactions $e^+e^- \to \nu\overline{\nu}W^+W^-$ and $e^+e^- \to \nu\overline{\nu}ZZ$. We describe the results that Barger *et al.* [90] have obtained by analyzing these processes.

Barger *et al.* use several models to test the effectiveness of their analysis of $e^+e^- \to \nu\overline{\nu}W^+W^-$ and $\nu\overline{\nu}ZZ$. In addition to the Standard Model Higgs boson with mass $m_H =$ 1 TeV, they use a Chirally–Coupled Scalar (CCS) model, a Chirally–Coupled Vector (CCV) model, and the LET model. They utilize a series of cuts to produce an event sample that is rich in the final states $\nu\overline{\nu}W_{\rm L}^+W_{\rm L}^-$ and $\nu\overline{\nu}Z_LZ_L$. Figure 2.43 shows the M_{WW} and M_{ZZ} distributions after all cuts. The 1 TeV Higgs scalar resonance stands out in both the $\nu\overline{\nu}WW$

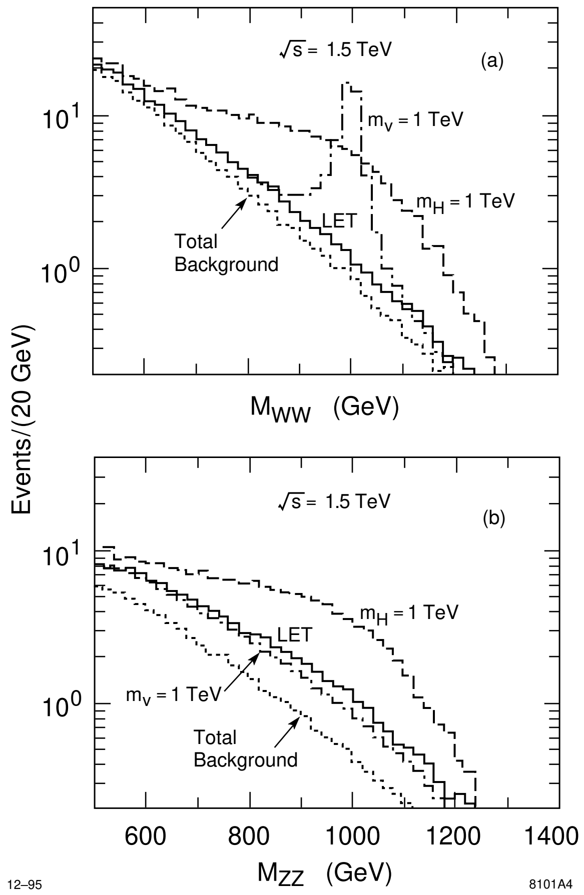

Figure 2.43: Expected numbers of W^+W^-, $ZZ \to (jj)(jj)$ signal and background events after all cuts for 200 fb^{-1} luminosity at $\sqrt{s} = 1.5$ TeV: (a) $e^+e^- \to \nu\overline{\nu}W^+W^-$, (b) $e^+e^- \to \nu\overline{\nu}ZZ$. The dotted histogram shows total SM background. The solid, dashed and dot–dashed histograms show signal plus background for the LET, SM, and CCV models, respectively; CCS model results are close to the SM case.

and $\nu\overline{\nu}ZZ$ final states. The 1 TeV vector resonance is prominent in the M_{WW} distribution (of course such a resonance would have been seen earlier as a 16σ signal at $\sqrt{s} = 0.5$ TeV, in $e^+e^- \to W^+W^-$). The LET signal is larger for the final state $\nu\overline{\nu}ZZ$ than it is for $\nu\overline{\nu}WW$.

The statistical significance of the signals for the different models is given in Table 2.8 assuming 100% initial-state e^- polarization at $\sqrt{s} = 1.5$ TeV and 200fb^{-1} luminosity. Note that the statistical significance of the LET signal is 8.5σ in the $\nu\overline{\nu}ZZ$ channel.

The $I = 2$ Goldstone boson scattering channel can be probed at the NLC through the reaction $e^-e^- \to \nu\nu W^-W^-$. Barger *et al.* [91] have studied this reaction and they obtain

Table 2.8: Signal and background for $e^+e^- \to \nu\overline{\nu}W^+W^-$ and $e^+e^-\nu\overline{\nu}ZZ$ with 100% initial state electron polarization, from Ref. [90].

Signal (S) or Background (B)	SM $M_H = 1$ TeV	Scalar $M_S = 1$ TeV	Vector $M_V = 1$ TeV	LET
$S(e^+e^- \to \nu\overline{\nu}W^+W^-)$	330	320	92	62
B(backgrounds)	280	280	7.1	280
$S/\sqrt{B}$	20	20	35	3.7
$S(e^+e^- \to \nu\overline{\nu}ZZ)$	240	260	72	90
B(backgrounds)	110	110	110	110
$S/\sqrt{B}$	23	25	6.8	8.5

Table 2.9: Signal and background for $e^-e^- \to \nu\overline{\nu}W^-W^-$ with 100% initial state electron polarization, from Ref. [91].

Signal (S) or Background (B)	SM $M_H = 1$ TeV	Scalar $M_S = 1$ TeV	Vector $M_V = 1$ TeV	LET
$S(e^-e^- \to \nu\overline{\nu}W^-W^-)$	110	140	140	170
B(backgrounds)	710	710	710	710
$S/\sqrt{B}$	4.0	5.2	5.4	6.3

the statistical significances shown in Table 2.9. An initial state electron polarization of 100% has been assumed for both beams.

2.7.3 The Reaction $e^+e^- \to \nu\overline{\nu}t\overline{t}$

If there is no light Higgs boson, the process $t\overline{t} \to W^+W^-$ violates unitarity in the multi-TeV energy region. It is natural then to ask if strong symmetry breaking can be detected through the process $W^+W^- \to t\overline{t}$. This process would be studied at the NLC by observing the reaction $e^+e^- \to \nu\overline{\nu}t\overline{t}$.

The total cross sections for $e^+e^- \to e^+e^-t\overline{t}$ and $e^+e^- \to \nu\overline{\nu}t\overline{t}$ have been calculated by Kauffman [92] for an e^+e^- center-of-mass energy of 2 TeV (Fig. 2.44). The cross sections for $\sqrt{s} = 1.5$ TeV should be similar. For $\sqrt{s} = 2$ TeV and 200 fb^{-1} luminosity we would have 1200 events from $e^+e^- \to e^+e^-t\overline{t}$ and 60 (400) events from $e^+e^- \to \nu\overline{\nu}t\overline{t}$ for $m_H =$ 0.1 (1.0) TeV. A 1 TeV Higgs boson therefore produces a 30% increase in the sum of the

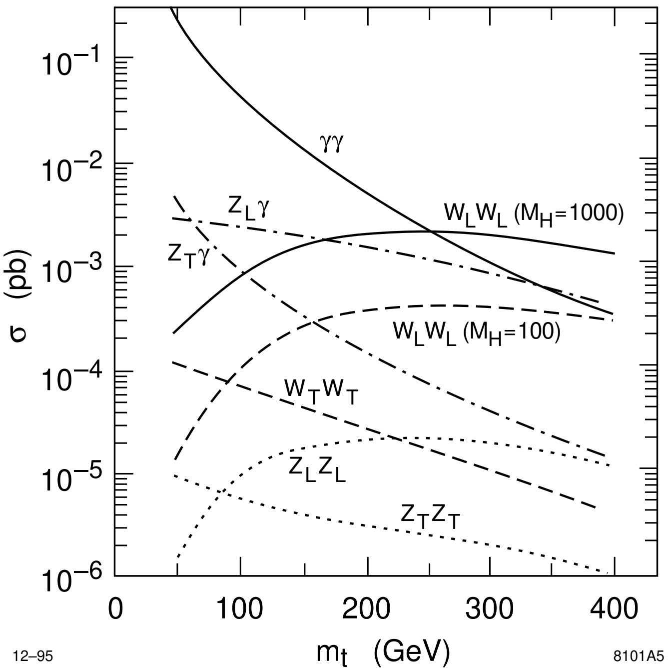

Figure 2.44: Contributions from various subprocesses to the total cross sections for $e^+e^- \to e^+e^- t\bar{t}$ and $e^+e^- \to \nu\bar{\nu}t\bar{t}$. The contributions are plotted as a function of the top quark mass m_t. The e^+e^- center-of-mass energy is 2 TeV.

cross sections for $e^+e^- \to e^+e^- t\bar{t}$ and $e^+e^- \to \nu\bar{\nu}t\bar{t}$ before any cuts are applied. The same 1 TeV Higgs boson produces only a 0.3% increase in the sum of the cross sections for $e^+e^- \to e^+e^- W^+W^-$ and $e^+e^- \to \nu\bar{\nu}W^+W^-$.

The strong symmetry breaking signal can be further enhanced by performing a helicity analysis on the $t\bar{t}$ final state to isolate the polarization states $t_L\bar{t}_L$ and $t_R\bar{t}_R$ corresponding to helicity-flip pair production. This can be done by observing the W energy distribution in t decays. Projecting out these helicity combinations would be the analog of projecting out the $W_{\rm L}^+W_{\rm L}^-$ and Z_LZ_L final states in gauge boson scattering.

2.7.4 Statistical significances at LHC versus NLC

The statistical significances of strong symmetry breaking signals at the NLC and LHC are summarized in Table 2.10. The LHC results are taken from the ATLAS design report [24]. If an entry is blank it may mean that the process is insensitive to the corresponding model or that the analysis has not been done; no distinction is made between the two possibilities. The entries for the direct gauge boson scattering processes at the NLC ($W^+W^- \to ZZ$ and $W^-W^- \to W^-W^-$) assume that the electron beam always has 90% left–handed polarization. For both the NLC and LHC results it was assumed that the 1.5 TeV technirho had a width of 0.33 TeV.

Table 2.10: Statistical significances of strong symmetry breaking signals at the NLC and LHC.

Collider	Process	$\sqrt{s}$ (TeV)	$\mathcal{L}$ (fb^{-1})	$M_\rho =$ 1.5 TeV	$M_H =$ 1 TeV	LET
NLC	$e^+e^- \to W^+W^-$	.5	80	7σ	–	–
NLC	$e^+e^- \to W^+W^-$	1.0	200	35σ	–	–
NLC	$e^+e^- \to W^+W^-$	1.5	190	366σ	–	5σ
NLC	$W^+W^- \to ZZ$	1.5	190	–	22σ	8σ
NLC	$W^-W^- \to W^-W^-$	1.5	190	–	4σ	6σ
LHC	$W^+W^- \to W^+W^-$	14	100	–	14σ	–
LHC	$W^+W^+ \to W^+W^+$	14	100	–	3σ	6σ
LHC	$W^+Z \to W^+Z$	14	100	7σ	–	–

Some points about Table 2.10 are worth noting:

1. Although the LHC can access larger W^+W^- center-of-mass energies, the statistical significance of the NLC signal is always larger. In most cases, this is a small effect, but it makes a significant point: Electron beam polarization, smaller backgrounds, and the utilization of the full e^+e^- center-of-mass energy for vector resonances has allowed the NLC to more than make up for its lower range of W^+W^- center-of-mass energies.

2. The NLC has a special ability to detect vector resonances. At $\sqrt{s} = 500$ GeV the technirho mass reach of the NLC is equal to that of the LHC. At $\sqrt{s} = 1500$ GeV the NLC is sensitive to strong interaction effects in $I = J = 1$ W^+W^- scattering even when they are nonresonant.

3. Signal significances for $W^+W^- \to t\bar{t}$ were not included in Table 2.10 because detector simulations have not yet been performed. From the discussion in Section 2.7.3, however, it appears that this is a promising reaction for the study of strong symmetry breaking at the NLC. It is probably very difficult to study $W^+W^- \to t\bar{t}$ at LHC due to the large background from $gg \to t\bar{t}$.

Finally it is important to remember that the significances shown in Table 2.10 include statistical errors only. Systematic errors have largely been ignored in analyses so far, both for the LHC and for the NLC.

2.7.5 Conclusion

An e^+e^- linear collider with $\sqrt{s} = 500 - 1500$ GeV would be an effective partner to the LHC in the study of strong symmetry breaking. It provides important complementary capabilities for the discovery of vector resonances and the extraction of chiral Lagrangian parameters. The NLC and LHC are expected to have similar statistical errors for scalar resonance and non–resonant signals in gauge boson scattering; however, the physics environments at the two machines are very different, and the systematic errors for the NLC analyses are probably smaller. The NLC is probably the only machine that can study $W^+W^- \to t\bar{t}$.